Prevention of brain damage after traumatic brain injury by pharmacological enhancement of KCNQ (Kv7, "M-type") K^+ currents in neurons

Fabio A. Vigil[1]*, Eda Bozdemir[2]*, Vladislav Bugay[1], Sang H. Chun[2], MaryAnn Hobbs[1], Isamar Sanchez[1], Shayne D. Hastings[1], Rafael J. Veraza[1], Deborah M. Holstein[2], Shane M. Sprague[3], Chase M. Carver[1], Jose E. Cavazos[4], Robert Brenner[1], James D. Lechleiter[2] and Mark S. Shapiro[1]

[1]Departments of Cellular and Integrative Physiology, [2]Cell Systems and Anatomy, [3]Neurosurgery, and [4]Neurology at the University of Texas Health San Antonio, Texas, USA, 78229.

*These authors contributed equally to this work.

SUPPLEMENTARY MATERIALS AND METHODS

Electroencephalogram

To quantify seizure frequency and determine seizure susceptibility, mice of each cohort were implanted with EEG electrodes 24 hours after CCCI or sham. A headmount was attached to a reference and 3 lead screws, 0.10'' and 0.12,'' connected to a preamplifier (Gain 25X) (Pinnacle Technologies). The 3 leads were inserted over the right frontal and right and left parietal cortical areas, and the reference electrode was inserted over the left frontal cortical area. The headmount and electrodes were further secured to the skull with dental cement (Lang Dental). The Stellate Harmonie acquisition hardware and software used to collect coincident video images of the animals with EEG activity and had several automated seizure detection algorithms.

Lactate/Pyruvate quantification

For lactate and pyruvate quantification, mouse brains were bathed in ice-cold Ringer's solution and maintained over ice during dissection of cortical and cerebellar samples. Ipsilateral samples collected were from tissue of 2 mm x 2 mm squares dissected around the impact area (Supplementary Fig. 1). The samples contained all cortical layers; hence, the 2 mm^3 cube-shaped volume sample was level with the cortex in the dissected area. The contralateral cortical samples were collected in the corresponding area to that in the ipsilateral hemisphere. For the sham cohort, similar samples were collected from both hemispheres between the rostral and middle branches of the superior sagittal sinus, visible by eye, to where our TBI model was always localized (Supplementary Fig. 1). The cerebellum was also isolated and divided into contralateral and ipsilateral hemispheres. Since the right hemisphere was always the side to receive a CCCI, "ipsilateral" measurement was always from the right hemisphere. All samples were homogenized immediately after collection with lactate assay buffer (BioVision) and centrifuged at 4 °C, 2,000 g for 10 minutes. Supernatants were collected, and proteins removed by additional centrifugation at 4 °C, 13,000 g for 10 min through 10 kD polyethersulfone spin filter columns (Thermo Fisher Scientific). Proteins were removed from the samples to prevent enzymatic degradation of lactate and/or pyruvate. Samples were frozen at -80 °C for future analysis.

Cell Death and blood-brain barrier permeability

PSVue794, a near infra-red (NIR) fluorescent probe, was used to visualize apoptosis and necrosis. Briefly, PSVue794 (Molecular Targeting) was prepared the day of the experiment. At 3 mg/kg, PSVue 794 was injected through the lateral tail vein at 24h post-TBI and imaging delayed for 48 h to ensure to minimize non-targeted probe retention effect around peripheral tissues. At 72 h post-TBI, mice were euthanized and transcardial perfusion performed to wash out

intravascular PSVue794. The entire brain was dissected from the skull, briefly kept in ice-cold phosphate buffered saline (PBS), and then immediately placed into an IVIS Spectrum Imaging System (PerkinElmer). NIR fluorescence signals were detected *ex vivo* with the following settings: excitation filter, 710 nm; emission filter, 820 nm; exposure time, auto; binning, medium; f/stop, 2; field of view, A. as recommended in IVIS operation guide.

Evans Blue was used to assess BBB permeability. 72 hours after CCCI, mice were injected with 2.5 mg/kg Evans Blue (Sigma-Aldrich) through the lateral tail vein. The dye was allowed to circulate for 2 hours until the mice were euthanized and transcardial perfusion performed to wash out intravascular dye. The brain was dissected from the skull, briefly kept in ice-cold PBS, and then immediately placed into an IVIS Spectrum Imaging System (PerkinElmer). The same cohort of animals went through both PSVue794 and Evans Blue imaging. After PSVue794 imaging, brains were sliced with two sequential 2 mm sections (Sections A and B) around Bregma and further imaged to detect Evans blue extravasation. Imaging was performed for both faces (rostral and caudal) of each section. Evans Blue fluorescence signals were detected *ex vivo* with settings: excitation filter, 640 nm; emission filter, 680 nm; exposure time, auto; binning, medium; f/stop, 2; field of view, A. as recommended in IVIS operation guide.

The values obtained with both probes scale linearly with emission intensity, and care was taken not to saturate the camera. Subjects were masked by adaptive fluorescence background subtraction in order to discard instrument background as explained in Caliper Life Sciences Reference Guide. Graphical representations of the results obtained show Radiant efficiency (Emission Light (photons/sec/cm^2/steradian)/Excitation Light (μW/cm^2)) and values where divided by 10^6 (for PsVue 794) and 10^7 (for Evans Blue) for normalization of data. Evans Blue and PSVue 794 fluorescent signals were imaged independently but in the same animals, levels of BBB leakage and cell death were correlated to each other by means of a fit to a linear regression function.

Fluoro Jade B

Neuronal death was detected by Fluoro Jade B (FJB) staining. Six days after CCCI, mice were euthanized via transcardial perfusion with PBS followed by 4% (w/v) paraformaldehyde (PFA). Brains were removed, post-fixed overnight in 4% PFA (Electron Microscopy Sciences), transferred into 30 % (w/v) sucrose in PBS and kept at 4ºC for 3 days. Brains were then embedded into Peel-A-Way Disposable Histology Molds (TedPella) filled with Fisher Healthcare Tissue-Plus O.C.T. compound (Fisher Scientific), rapidly frozen with 2-methylbutane immersed in liquid N^2 and stored at -80 ºC until cryosectioning. Thirty (30) μM thick coronal sections within the parietal cortex were prepared using a HM 505E Cryostat (Microm International), mounted on Superfrost Plus microscope slides (Fisher Scientific) previously coated with gelatin (Sigma), and dried overnight. Slides were stored at -80 ºC until used. On the day of the experiment, all solutions were freshly prepared. Slides were kept in KPBS for 2 min and followed by dehydration steps in 50%-70%-100% ethanol for 2 min/each. Slides were rehydrated by repeating those steps in 70%-50% ethanol, KPBS 2 min each and incubated in potassium permanganate 0.06% for 5 min. After gentle rinsing in ddH_2O, slides were further incubated in Fluoro-Jade B (Sigma Aldrich) solution for 10 min and rinsed in ddH_2O 3X for 1 min/each. Stained slides were then dried, cleared in Xylene 3X each 2 min, and cover-slipped with DPX. A Nikon Eclipse Ti with camera coolSNAP HQ^2 microscope with 20X objective (N.A. 0.75) was used to take fluorescence images of FJB and counterstained DAPI. Fluorescence excitation-emission for Fluoro Jade and DAPI were 470/40-500lp and 350/50-460/50p, respectively. Cell count was obtained by non-biased automatic quantification with ImageJ/FIJI (NIH, USA). All settings and parameters were held constant. After background subtraction and image threshold (1.05 %), FJB positive cells were detected using the “analyze particles” (size: 20-100, circularity: 0.00-1.00) function of ImageJ. These parameters

determined pixel size and circularity of the acceptable ROIs and were used to identify cell bodies automatically.

Immunohistochemistry

Slices previously processed six days after CCCI were used for immunohistochemistry. Slices stored at -80 ºC on slides were brought to RT and dried overnight. The following day, they were rehydrated with PBS and their immunoreactivity enhanced via heat-induced antigen retrieval using DIVA decloaker (Biocare Medical). Slides were then washed with PBS twice for 5 min and dipped into 0.25 % (v/v) Triton X-100 (Sigma-Aldrich) for another 10 min. Following two more PBS washes, sections were blocked with 5 % (v/v) Bovine Serum Albumin (Sigma) for 1 hour at RT, excess blocking solution removed, and sections incubated with primary antibodies (1:1000 GFAP, Abcam ab53554; 1:500 Iba1, Wako 019-19741) at 4ºC for 20 hours. The following day, sections were washed with PBS 5X for 15 min/each and incubated in secondary antibodies (1:200 Thermo Fisher donkey anti-Goat Alexa Fluor 568; 1:200 Thermo Fisher, Chicken anti-Rabbit Alexa Fluor 488) for 1 hour at RT. They were then washed 3X for 5 min/each, and further incubated in DAPI (Sigma) for 10 min. After a brief wash in ddH_2O, slides were mounted with Vectashield antifade mounting medium (Vector Laboratories) and cover-slipped. All images were taken at 20X magnification (0.8 N.A.) using a Zeiss LSM710 confocal microscope.

Fluorescence settings and parameters were held constant during each measurement. Mean fluorescence intensity and corrected total cell fluorescence (CTCF) values were calculated using ImageJ. For CTCF, a single plane confocal image of the cerebral cortex was taken for both GFAP and Iba1 analysis, on each brain slice. The confocal plane used was selected based on the absence of holes or any other artifact. Each image underwent background subtraction. To identify cell bodies in the image (the ROIs), the desired binary images were generated by using the threshold option set at 5-15% for GFAP and 4-6% for Iba1 images. The following parameters were utilized to detect the ROIs automatically using the ImageJ function “analyze particles,” with size settings for GFAP and Iba1 at 40-8000 and 10-8000, respectively, and circularity of both GFAP and Iba1 at 0.0-10.0. With these parameters, ImageJ was able to automatically detect cell bodies and define them as ROIs. The mean gray value, integrated density, and ROI area were obtained along with background readings. CTCF was calculated by subtracting from the integrated density of each cell the area of the ROI multiplied by the mean fluorescence of background readings. As for the mean fluorescence intensity analysis, the stacked images at 1 µm intervals were taken from each brain section. A customized ImageJ plugin from the Indiana Center for Biological Microscopy (ICBM) was employed to mask the images. The mean fluorescence intensity of the cortical region was calculated using automatic detection of positive pixels by the ICMB plugin. The results obtained for mean fluorescence intensity of the image and CTCF were averaged for each animal. Each average was used independently for statistical analysis and are represented as dots in the corresponding dot plot graph.

For visualization and quantification of KCNQ2 transcription, we performed experiments on KCNQ2 mRNA-EGFP reporter mice (KCNQ2-EGFP/FW221Gsat/Mmucd, stock number 015412-UCD), in which mice are transgenic for a bacterial artificial chromosome (RP23-247P15) containing the KCNQ2 locus with EGFP inserted immediately upstream of the first axon coding sequence gene. These mice were established on a mixed background of FVB/N and Swiss Webster and maintained on a Swiss Webster background by mating hemizygous transgenic males with wildtype Swiss Webster females. Hemizygous male and female progeny of 2-3 months age were used for experiments. All mice were threated with RTG 30 min after injury and samples were collected 24h after CCCI. Slices (200 µm) were infused with 4 % (w/v) PFA for 10 min at RT, washed 5X in PBS and blocked with 8 % (v/v) donkey serum (Sigma-Aldrich) diluted in PBS, 0.1 % (v/v) Triton X-100 (Sigma-Aldrich), and 0.1 % (v/v) Tween 20 (Thermo Fisher Scientific). After blocking for 2 h at RT, slices were stained overnight at 4 ºC using an anti-EGFP antibody (1:2000; Rockland 600-101-215) and counterstained with anti-Microtubule associated protein 2

(MAP2) (1:5000, Abcam ab5392). We measured the immunofluorescence of anti-EGFP/FITC antibodies, instead of just EGFP fluorescence itself because previous work in the lab has demonstrated this method to yield a much lower signal/noise ratio. MAP2 was used as a counterstain to confirm neuron-specific expression of KCNQ2. For detection of primary antibodies, anti-goat IgG (1:150, FITC, Jackson ImmunoResearch) and anti-chicken IgG (1:400, Rodamine, Jackson ImmunoResearch) secondary antibodies were used. A Nikon Eclipse FN1 microscope with 10X and 40X Plan Fluor objectives was used for detection of fluorescence. Images were obtained at a fixed exposure time of 5 s (averaging 8 frames). Cell count, mean, and maximum fluorescence per cell were obtained by non-biased automatic quantification with ImageJ. The image threshold was set at 15-25% to facilitate ROI identification. ROIs were determined automatically again using the "analyze particles" function of ImageJ, with size set to 200-8000 and circularity set to 0.00-1.00.

Quantitative real-time polymerase chain reaction (qRT-PCR)

qRT-PCR was performed to quantify the mRNA levels of KCNQ2 and KCNQ3, 24 h and 6 days after CCCI. Cortical samples dissected as described in the section "Lactate/Pyruvate quantification," were snap frozen in dry ice and stored at -80°C until analysis. Samples were homogenized in TRIzol buffer (Life) using an Ultra EZgrind tissue homogenizer (Denville Scientific) at the lowest speed. After chloroform extraction, total RNA was precipitated and resuspended in nuclease-free water. RNA quality and quantity were tested, for each sample, using a spectrophotometer (Nanodrop). cDNAs were synthesized with SuperScript III first-strand (Invitrogen) following the manufacturer's protocol. Oligo$(dT)_{20}$ (Invitrogen) was used for mRNA specific amplification and 800 ng of total RNA used in each reaction. For amplification of KCNQ2, KCNQ3 and the housekeeping gene hypoxanthine phosphoribosyl transferase (HPRT) the primers used were KCNQ2: F- GGGGTCTGATCACCCTGACGA, R- GCCAGCAGGAAGAGCAAAGAACG; KCNQ3: F- AGCAGTCTCCAAGGAATGAACCA, R- CCCATGTCATGAACCTGTCTTTCAAC; HPRT: F- ATACAGGCCAGACTTTGTTGGATT, R- TCACTAATGACACAAACGTGATTCAA. qRT-PCR reactions were performed in a 7900 HT Fast Real-Time PCR system (Life Technologies). Each sample was run in triplicates for each primer. To confirm the specificity of primers, the amplicons obtained were run by electrophoresis in an agarose gel. Dilution of cDNA samples was determined by equal amplification efficiencies of both the template and HPRT over a range of cDNA dilutions. Optimum sample dilutions were defined as the mid-point in the line which the equation describing it had an "a" value smaller than 0.1. HPRT was chosen as housekeeping gene by comparing the efficiency of amplification of different dilutions of this primer to other possible housekeeping genes (β-Actin and GAPDH). The number of cycles necessary to use all the substrate in a reaction with ddH_2O was subtracted to the number of cycles obtained with a test sample. The larger the difference in the number of cycles, the higher the efficiency and specificity of the reaction. With a good primer, spurious amplification reaches the limit at 40 cycles in ddH_2O, but samples containing the template needs fewer cycles to exhaust the reaction, thus quantifying mRNA. The same procedure was performed throughout our experiments to determine the best concentrations of forward and reverse primers for KCNQ2, KCNQ3, and HPRT in each qRT-PCR reaction. qRT-PCR reactions were performed in a 7900 HT Fast Real-Time PCR system (Life Technologies) using SYBR Green PCR master mix (Thermo Fisher Scientific). The reaction started with one-step of 95°C for 10 minutes, followed by 40 cycles of 95°C for 15 seconds and 60°C for 1 minute. The number of cycles needed to reach exhaustion of the reaction, threshold cycle (CT), was determined. The difference between template CT and housekeeping gene CT (ΔCT) was calculated and transformed using a power of 2.

Statistical analysis

Video/EEG monitoring data were analyzed using Pearson chi-squared test as data was composed of dichotomous nominal variables. All other data were checked for normal distribution

by Q-Q plot analysis and the Shapiro-Wilk normality test. In cases of non-normal distribution, outliers were excluded from the experiment as a normalization strategy [132-134]. Outliers were defined as values that fall more than 1.5 times the interquartile range above the third quartile or below the first quartile [134, 135]. If data were still not normally distributed, then they were transformed to Log_{10} [136, 137]. Using these two procedures, normal distributions were observed in all the continuous data collected, except for the mean and maximum KCNQ2 mRNA-EGFP signals. Those data were analyzed using a Mann-Whitney U test. For normally distributed data, one-way ANOVA tests were used in experiments with only one independent variable. A two-way ANOVA test was used to analyze experiments with two independent variables. The two factors used were hemisphere (injured/Ipsilateral against non-injured/Contralateral) and cohort (Sham, TBI or TBI+RTG). Bonferroni tests were used for *post hoc* comparisons for determining significant differences between different groups of samples, once ANOVA revealed a significant difference. Non-significant results not presented in the main text of this article can be found in Supplementary Table 1 of the *Supplemental Material*.

Linear regression analysis was performed to test the relationship between two dependent variables collected in the same animal. To perform a linear regression analysis, the data must be collected within the same cohort of animals. Therefore, Evans blue and PSVue 794 were tested against each other. Additionally, immunoblotting semi-quantification of Iba1, CD40L, and RIP1 were tested against each other. As the collection of Evans blue and PSVue 794 fluorescence data required us to sacrifice the mice, it would be impossible to combine such an approach with the 5 days-long video/EEG recording performed here. We attempted to use samples from the EEG recording experiments for the immunoblotting analysis, but the EEG surgery procedure resulted in unacceptable increase in background for the Iba1 measurements, even in Sham animals. For linear regression analysis, values obtained in the three cohorts of animals (Sham, TBI, TBI+RTG) were always included.

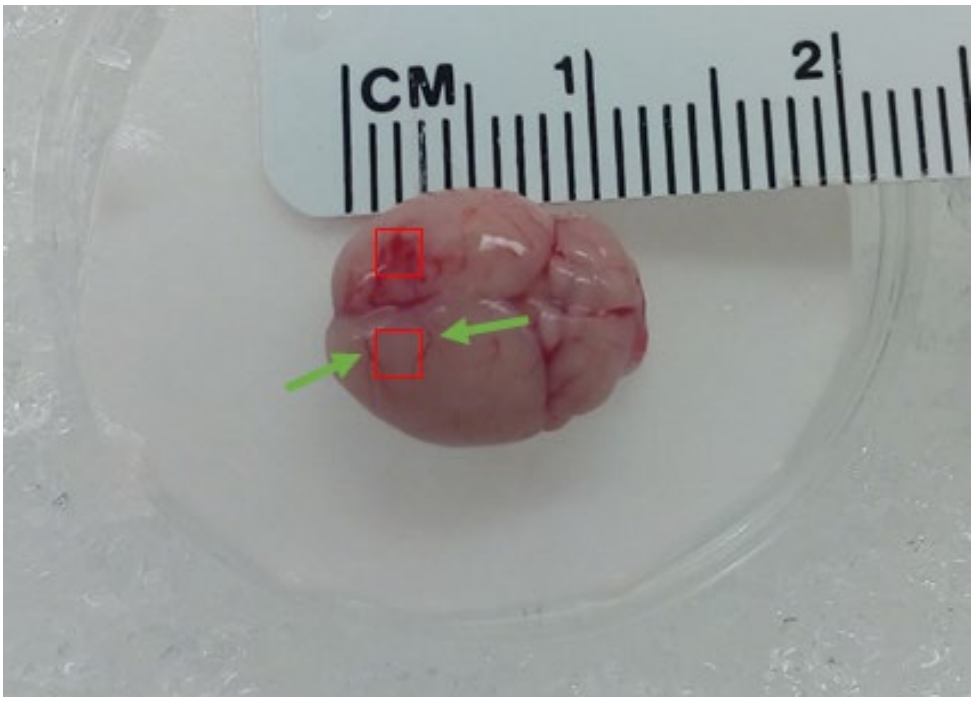

Supplementary Figure 1. Photo of mouse brain 24h after CCCI. The red box indicates cortical areas that were collected as samples in both ipsilateral and contralateral sides for the lactate and pyruvate quantification presented on Figs. 1C-D. Intense red regions can be seen in the hit area. Green arrows point to the first and second visible branches of the superior sagittal sinus. These two blood vessels, visible by eye, where used as reference for collection of Sham samples, for which red areas were not present.

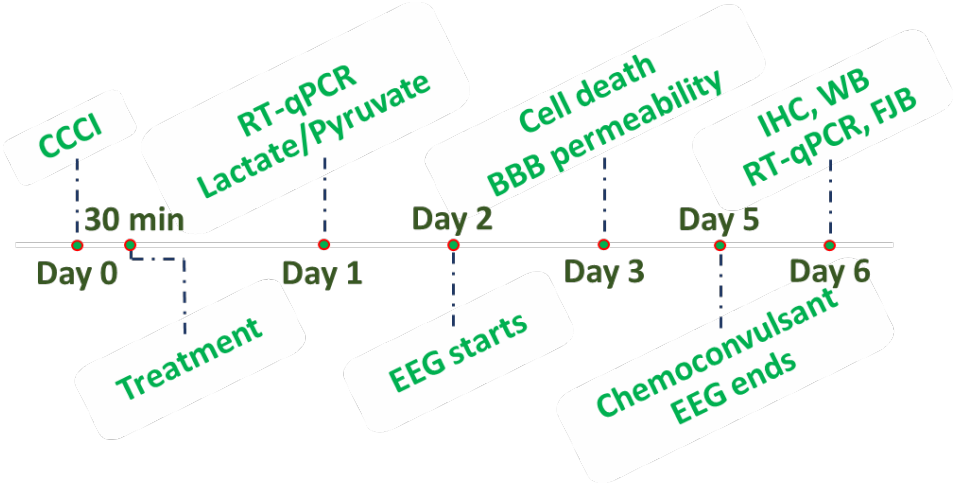

Supplementary Figure 2. Experimental design with timeline. This figure shows the experimental design for all the experiments performed in this work placed on a timeline. On day 0 animals were subjected to CCCI injury and administered either vehicle only or RTG. Samples were used for quantification of lactate and pyruvate levels and for qRT-PCR experiments collected 24h after injury. EEG/video recording was performed from days 2 to 5, with a chemoconvulsant challenge on day 5. BBB permeability and cell death were studied 3 days after TBI. Samples for histology (FJB), immunohistochemistry (IHC), immunoblotting (WB) and a second cohort of qRT-PCR samples were collected 6 days after CCCI.

SUPPLEMENTAL RESULTS

Supplementary Table 1. Gender-related effects

This table presents the statistical analysis looking for gender-related effects on our experiments. Three-way ANOVA was performed. Factors were hemisphere (ipsilateral or contralateral), treatment group (Sham, TBI, or TBI+RTG), and gender (female or male). No significant gender effect was observed.

Data	Three-way ANOVA	Gender	Mean ± S.D.
Lactate/pyruvate ratio (Cortex)	-Effect of gender: $F_{1,30}$=1.8; p=0.40 -Gender vs Hemisphere interaction effect: $F_{1,30}$=0.8; p=0.36 -Gender vs Group interaction effect: $F_{2,30}$=0.1; p=0.98 -Gender vs Hemisphere vs Group interaction effect: $F_{2,30}$=0.1; p=0.87	Male	Ipsilateral: -Sham: 9.32 ± 3.02 -TBI: 16.10 ± 7.06 -TBI+RTG: 9.10 ± 1.29 Contralateral: -Sham: 7.84 ± 2.73 TBI: 5.88 ± 4.46 TBI+RTG: 8.70 ± 2.83
		Female	Ipsilateral: -Sham: 3.92 ± 0.77 -TBI: 10.7527 ± 0.0001 -TBI+RTG: 2.65 ± 3.10 Contralateral: -Sham: 3.58 ± 4.36 -TBI: 2.63 ± 0.40 -TBI+RTG: 6.62 ± 2.45
Lactate/pyruvate ratio (Cerebellum)	-Effect of gender: $F_{1,34}$=1.7; p=0.21 -Gender vs Hemisphere interaction effect: $F_{1,34}$=0.6; p=0.41 -Gender vs Group interaction effect: $F_{2,34}$=2.2; p=0.12 -Gender vs Hemisphere vs Group interaction effect: $F_{2,34}$=0.9; p=0.41	Male	Ipsilateral: -Sham: 42.13 ± 13.30 -TBI: 25.62 ± 11.47 -TBI+RTG: 21.49 ± 9.24 Contralateral: -Sham: 22.38 ± 4.47 -TBI: 29.84 ± 10.59 -TBI+RTG: 19.12 ± 7.39
		Female	Ipsilateral: -Sham: 24.26 ± 12.63 -TBI: 15.46 ± 1.21 -TBI+RTG: 28.03 ± 7.56 Contralateral: -Sham: 22.56 ± 10.42 -TBI: 20.23 ± 5.51 -TBI+RTG: 23.87 ± 10.84
Immunoblotting Iba1	-Effect of gender: $F_{1,77}$=1.0; p=0.31 -Gender vs Hemisphere interaction effect: $F_{1,77}$=0.1; p=0.71 -Gender vs Group interaction effect: $F_{2,77}$=1.2; p=0.31	Male	Ipsilateral: -Sham: 0.91 ± 0.37 -TBI: 1.20 ± 0.35 TBI+RTG:0.96 ± 0.20 Contralateral: -Sham: 0.63 ± 0.53 -TBI: 0.72 ± 0.38 -TBI+RTG: 0.86 ± 0.43

	-Gender vs Hemisphere vs Group interaction effect: $F_{2,77}$=1.0; p=0.35	Female	Ipsilateral: -Sham: 0.47 ± 0.31 -TBI: 1.49 ± 0.52 -TBI+RTG: 0.92 ± 0.44 Contralateral: -Sham: 0.52 ± 0.41 -TBI: 0.62 ± 0.20 -TBI+RTG: 0.66 ± 0.35
Immunoblotting CD40L	-Effect of gender: $F_{1,73}$=0.1; p=0.76 -Gender vs Hemisphere interaction effect: $F_{1,73}$=0.002; p=0.96 -Gender vs Group interaction effect: $F_{2,73}$=1.1; p=0.32 -Gender vs Hemisphere vs Group interaction effect: $F_{2,73}$=0.1; p=0.91	Male	Ipsilateral: -Sham: -0.018 ± 0.398 -TBI: 0.131 ± 0.068 -TBI+RTG: -0.177 ± 0.514 Contralateral: -Sham: -0.146 ± 0.213 -TBI: -0.172 ± 0.197 -TBI+RTG: -0.312 ± 0.208
		Female	Ipsilateral: -Sham: -0.137 ± 0.228 -TBI: 0.121 ± 0.094 -TBI+RTG: 0.0021 ± 0.3116 Contralateral: -Sham: -0.169 ± 0.0932 -TBI: -0.214 ± 0.224 -TBI+RTG: -0.177 ± 0.288
Immunoblotting RIP1	-Effect of gender: $F_{1,86}$=1.3; p=0.24 -Gender vs Hemisphere interaction effect: $F_{1,86}$=0.02; p=0.88 -Gender vs Group interaction effect: $F_{2,86}$=0.4; p=0.95 -Gender vs Hemisphere vs Group interaction effect: $F_{2,86}$=0.2; p=0.84	Male	Ipsilateral: -Sham: 0.819 ± 0.384 -TBI: 1.19 ± 0.27 -TBI+RTG: 1.01 ± 0.31 Contralateral: -Sham: 0.826 ± 0.269 -TBI: 0.857 ± 0.160 -TBI+RTG: 1.01 ± 0.40
		Female	Ipsilateral: -Sham: 0.773 ± 0.311 TBI: 1.07 ± 0.35 TBI+RTG: 0.938 ± 0.505 Contralateral: -Sham: 0.698 ± 0.294 -TBI: 0.841 ± 0.335 -TBI+RTG: 0.847 ± 0.413
qRT-PCR KCNQ2 mRNA (24h after CCCI)	-Effect of gender: $F_{1,55}$=0.4; p=0.43 -Gender vs Hemisphere interaction effect: $F_{1,55}$=0.3; p=0.59 -Gender vs Group interaction effect: $F_{2,55}$=1.2; p=0.31 -Gender vs Hemisphere vs Group interaction effect: $F_{2,55}$=0.5; p=0.95	Male	Ipsilateral: -Sham: 0.359 ± 0.116 -TBI: 0.421 ± 0.098 -TBI+RTG: 0.485 ± 0.106 Contralateral: -Sham: 0.286 ± 0.0870 -TBI: 0.381 ± 0.079 -TBI+RTG: 0.392 ± 0.049
		Female	Ipsilateral: -Sham: 0.471 ± 0.184 -TBI: 0.478 ± 0.074 -TBI+RTG: 0.520 ± 0.013 Contralateral: -Sham: 0.392 ± 0.0618 -TBI: 0.398 ± 0.068 -TBI+RTG: 0.390 ± 0.0378
qRT-PCR KCNQ3 mRNA (24h after CCCI)	-Effect of gender: $F_{1,54}$=0.5; p=0.32 -Gender vs Hemisphere interaction effect: $F_{1,54}$=0.03; p=0.87	Male	Ipsilateral: -Sham: 0.246 ± 0.028 -TBI: 0.246 ± 0.049 -TBI+RTG: 0.255 ± 0.031

	-Gender vs Group interaction effect: $F_{2,54}$=1.7; p=0.18 -Gender vs Hemisphere vs Group interaction effect: $F_{2,54}$=0.6; p=0.55		Contralateral: -Sham: 0.221 ± 0.052 -TBI: 0.243 ± 0.072 -TBI+RTG: 0.244 ± 0.028
		Female	Ipsilateral: -Sham: 0.272 ± 0.024 -TBI: 0.296 ± 0.034 -TBI+RTG: 0.269 ± 0.040 Contralateral: -Sham: 0.275 ± 0.040 -TBI: 0.294 ± 0.057 -TBI+RTG: 0.217 ± 0.047
qRT-PCR KCNQ2 mRNA (6 days after CCCI)	-Effect of gender: $F_{1,47}$=0.2; p=0.66 -Gender vs Hemisphere interaction effect: $F_{1,47}$=0.007; p=0.93 -Gender vs Group interaction effect: $F_{2,47}$=0.5; p=0.60 -Gender vs Hemisphere vs Group interaction effect: $F_{2,47}$=0.6; p=0.57	Male	Ipsilateral: -Sham: 0.320 ± 0.125 -TBI: 0.393 ± 0.053 -TBI+RTG: 0.650 ± 0.184 Contralateral: -Sham: 0.482 ± 0.154 -TBI: 0.439 ± 0.174 TBI+RTG: 0.509 ± 0.064
		Female	Ipsilateral: -Sham: 0.359 ± 0.060 -TBI: 0.438 ± 0.206 -TBI+RTG: 0.521 ± 0.153 Contralateral: -Sham: 0.417 ± 0.072 -TBI: 0.455 ± 0.166 -TBI+RTG: 0.492 ± 0.047
qRT-PCR KCNQ3 mRNA (6 days after CCCI)	-Effect of gender: $F_{1,49}$=1.3; p=0.26 -Gender vs Hemisphere interaction effect: $F_{1,49}$=0.1; p=0.74 -Gender vs Group interaction effect: $F_{2,49}$=1.2; p=0.30 -Gender vs Hemisphere vs Group interaction effect: $F_{2,49}$=2.5; p=0.10	Male	Ipsilateral: -Sham: 0.113 ± 0.016 -TBI: 0.101 ± 0.037 -TBI+RTG: 0.167 ± 0.065 Contralateral: -Sham: 0.119 ± 0.014 -TBI: 0.120 ± 0.028 -TBI+RTG: 0.131 ± 0.019
		Female	Ipsilateral: -Sham: 0.128 ± 0.029 -TBI: 0.156 ± 0.072 -TBI+RTG: 0.126 ± 0.058 Contralateral: -Sham: 0.108 ± 0.017 -TBI: 0.144 ± 0.028 -TBI+RTG: 0.170 ± 0.039
Spontaneous seizure (EEG/Video)	**Pearson chi-square test*** $\chi(1) = 0.4$, p=0.52	Male	-TBI: 4 out of 11 -TBI+RTG: 0 out of 6
		Female	-TBI: 1 out of 4 -TBI+RTG: 0 out of 4
Pilocarpine induced spike activity (EEG)	**Pearson chi-square test*** $\chi(1) = 1.7$, p=0.19	Male	-TBI: 7 out of 9 -TBI+RTG: 1 out of 6
		Female	-TBI: 1 out of 4 -TBI+RTG: 1 out of 4

*Since these data were from dichotomous nominal variables Pearson chi-square test was used to probe for gender-related effects.

Supplementary Table 2. Non-significant results

Non-significant results that were not presented in the main article can be found in this table. This table contains results related to all the figures in the article.

Data	Statistical Test	Groups	Result
Lactate/pyruvate ratio (Cortex)	Two-way ANOVA (effect of group)	Sham; TBI; TBI+RTB	$F_{2,29}$=2.0; p=0.15
	Bonferroni *post-hoc*	Sham ipsi. X Sham cont.	t=0.02; p=0.98
		TBI+RTG ipsi. X TBI+RTG cont.	t=0.4; p=0.63
		Sham cont. X TBI cont.	t=0.6; p=1.0
		Sham cont. X TBI+RTG cont.	t=0.6; p=1.0
		TBI cont. X TBI+RTG cont.	t=1.2; p=0.62
Lactate/pyruvate ratio (Cerebellum)	Two-way ANOVA (effect of group)	Sham; TBI; TBI+RTB	$F_{2,34}$=0.7; p=0.48
	Two-way ANOVA (effect of hemisphere)	Contralateral x Ipsilateral	$F_{1,34}$=0.8; p=0.37
	Two-way ANOVA (interaction effect)	Group x Hemisphere	$F_{2,34}$=1.5; p=0.23
Evans Blue	Bonferroni *post-hoc*	TBI X TBI+RTG Slice A rostral	t=0.6; p=1.0
		TBI X TBI+RTG Slice B caudal	t=0.7; p=1.0
Correlation IVIS	Linear regression	PSVue 794 X Evans blue Slice A rostral	$F_{1,15}$=3.1; p=0.09
Immunoblotting Iba1	Bonferroni *post-hoc*	Sham ipsi. X TBI+RTG ipsi.	t=2.4; p=0.05
		Sham ipsi. X Sham cont.	t=1.2; p=0.22
		TBI+RTG ipsi. X TBI+RTG cont.	t=0.4; p=0.63
		Sham cont. X TBI cont.	t=0.8; p=1.0

		Sham cont. X TBI+RTG cont.	t=1.3; p=0.53
		TBI cont. X TBI+RTG cont.	t=0.5; p=1.0
Immunoblotting CD40L	Two-way ANOVA (effect of group)	Sham; TBI; TBI+RTB	$F_{2,72}$=1.7; p=0.17
	Two-way ANOVA (interaction effect)	Group X Brain Hemi.	$F_{2,72}$=1.3; p=0.25
	Bonferroni *post-hoc*	Sham ipsi. X Sham cont.	t=0.5; p=0.61
		Sham ipsi. X TBI+RTG ipsi.	t=0.1; p=1.0
		Sham ipsi. X TBI ipsi.	t=2.0; p=0.13
		TBI ipsi. X TBI+RTG ipsi.	t=2.0; p=0.12
		Sham cont. X TBI+RTG cont.	t=0.8; p=1.0
		Sham cont. X TBI cont.	t=0.2; p=1.0
		TBI cont. X TBI+RTG cont.	t=0.5; p=1.0
Immunoblotting RIP-1	Two-way ANOVA (effect of hemisphere)	Contralateral x Ipsilateral	$F_{1,85}$=3.0; p=0.08
	Two-way ANOVA (interaction effect)	Group X Brain Hemi.	$F_{2,85}$=1.1; p=0.32
	Bonferroni *post-hoc*	Sham ipsi. X Sham cont.	t=0.3; p=0.71
		Sham ipsi. X TBI+RTG ipsi.	t=1.4; p=0.46
		TBI ipsi. X TBI+RTG ipsi.	t=1.3; p=0.52
		Sham cont. X TBI+RTG cont.	t=1.4; p=0.47

		Sham cont. X TBI cont.	t=0.8; p=1.0
		TBI cont. X TBI+RTG cont.	t=0.5; p=1.0
Immunohistochemistry Iba1 – Mean fluorescence intensity	Bonferroni *post-hoc*	Sham cont. X TBI+RTG cont.	t=2.5; p=0.05
		TBI cont. X TBI+RTG cont.	t=1.9; p=0.21
		Sham ipsi. X Sham cont.	t=0.07; p=0.94
		TBI+RTG ipsi. X TBI+RTG cont.	t=0.5; p=0.60
Immunohistochemistry Iba1 – CTCF	Two-way ANOVA (effect of hemisphere)	Contralateral x Ipsilateral	$F_{1,27}$=0.4; p=0.51
	Two-way ANOVA (interaction effect)	Group X Brain Hemi.	$F_{2,27}$=0.9; p=0.41
	Bonferroni *post-hoc*	Sham cont. X TBI+RTG cont.	t=0.9; p=1.0
		TBI cont. X TBI+RTG cont.	t=1.7; p=0.26
		Sham ipsi. X TBI+RTG ipsi.	t=1.0; p=0.96
		Sham ipsi. X Sham cont.	t=0.2; p=0.82
		TBI ipsi. X TBI cont.	t=1.4; p=0.17
		TBI+RTG ipsi. X TBI+RTG cont.	t=0.16; p=0.87
Immunohistochemistry GFAP - Mean fluorescence intensity	Bonferroni *post-hoc*	TBI cont. X TBI+RTG cont.	t=0.5; p=1.0
		Sham ipsi. X Sham cont.	t=0.1; p=0.85
		TBI+RTG ipsi. X TBI+RTG cont.	t=1.3; p=0.18
Immunohistochemistry GFAP – CTCF	Two-way ANOVA (effect of hemisphere)	Contralateral x Ipsilateral	$F_{1,38}$=0.9; p=0.33
	Two-way ANOVA (interaction effect)	Group X Brain Hemi.	$F_{2,38}$=1.0; p=0.36

	Bonferroni *post-hoc*	Sham cont. X TBI+RTG cont.	t=1.0; p=0.89
		Sham ipsi. X TBI+RTG ipsi.	t=1.7; p=0.27
		Sham ipsi. X Sham cont.	t=0.3; p=0.75
		TBI ipsi. X TBI cont.	t=1.6; p=0.11
		TBI+RTG ipsi. X TBI+RTG cont.	t=0.3; p=0.76
qRT-PCR KCNQ2 mRNA (24h after CCCI)	Two-way ANOVA (effect of group)	Sham; TBI; TBI+RTG	$F_{2,54}$=2.2; p=0.11
	Two-way ANOVA (interaction effect)	Group X Brain Hemi.	$F_{2,54}$=0.2; p=0.75
	Bonferroni *post-hoc*	Sham ipsi. X Sham cont.	t=1.7; p=0.08
		Sham ipsi. X TBI+RTG ipsi.	t=1.7; p=0.23
		Sham ipsi. X TBI ipsi.	t=0.7; p=1.0
		TBI ipsi. X TBI+RTG ipsi.	t=1.0; p=0.86
		Sham cont. X TBI+RTG cont.	t=1.1; p=0.79
		Sham cont. X TBI cont.	t=1.1; p=0.75
		TBI cont. X TBI+RTG cont.	t=0.03; p=1.0
		TBI ipsi. X TBI cont.	t=1.3; p=0.16
qRT-PCR KCNQ3 mRNA (24h after CCCI)	Two-way ANOVA (effect of group)	Sham; TBI; TBI+RTG	$F_{2,49}$=2.4; p=0.10
	Two-way ANOVA (effect of hemisphere)	Contralateral x Ipsilateral	$F_{1,49}$=0.01; p=0.91
	Two-way ANOVA (interaction effect)	Group X Brain Hemi.	$F_{2,49}$=0.7; p=0.93
qRT-PCR KCNQ2 mRNA (6 after days)	Two-way ANOVA (effect of hemisphere)	Contralateral x Ipsilateral	$F_{1,46}$=0.08; p=0.76
	Two-way ANOVA (interaction effect)	Group X Brain Hemi.	$F_{2,46}$=2.4; p=0.09
	Bonferroni *post-hoc*	Sham ipsi. X Sham cont.	t=1.6; p=0.10
		Sham ipsi. X TBI ipsi.	t=1.1; p=0.76
		Sham ipsi. X TBI+RTG ipsi.	t=1.4; p=0.46
		TBI+RTG ipsi. X TBI ipsi.	t=1.5; p=0.43
		Sham ipsi. X Sham cont.	t=0.09; p=0.92
		TBI ipsi. X TBI cont.	t=0.6; p=0.53
		TBI+RTG ipsi. X TBI+RTG cont.	t=0.1; p=0.85
qRT-PCR KCNQ3 mRNA (6 after days)	Two-way ANOVA (effect of group)	Sham; TBI; TBI+RTB	$F_{2,49}$=2.4; p=0.10
	Two-way ANOVA (effect of hemisphere)	Contralateral x Ipsilateral	$F_{1,49}$=0.01; p=0.91
	Two-way ANOVA (interaction effect)	Group x Hemisphere	$F_{2,49}$=0.7; p=0.92

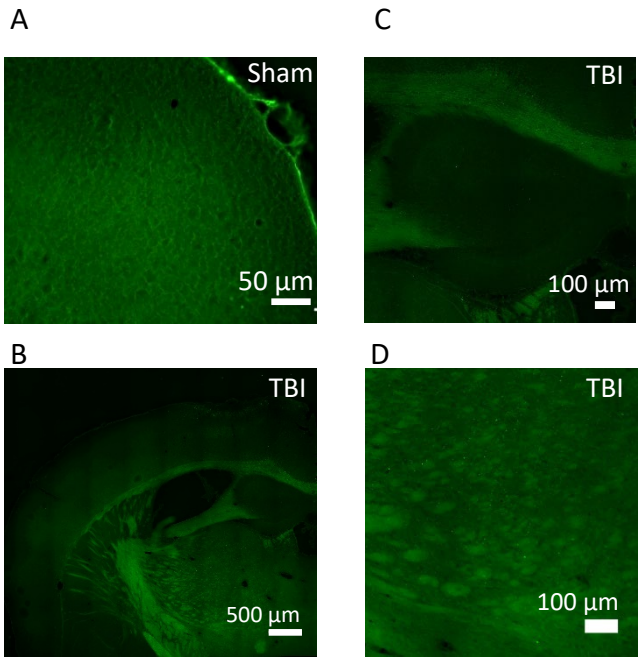

Supplementary Figure 3. FJB fluorescent staining shows lack of cell death in Sham mouse cortical slices and very weak and sparse signal in subcortical regions of TBI mice. (A) Representative image showing the lack of FJB stanning (green) in samples from Sham animals. This is predicted, as necrosis is not expected to be observed in the brains of Sham mice. **(B)** Exemplary image of FJB staining in a slice of a TBI animal. Panels **(C)** and **(D)** show amplification of the image in panel **(B)** focusing on the Hippocampus and Corpus Callosum **(C)** and in the striatum **(D)**. As can be seen in the images, FJB-positive staining can be observed in subcortical regions (small bright spots) like the ones seen above. However, the signal observed is very sparse and the signal-to-background ratio is very low. Hence, we were unable to quantify FJB staining in those regions. Experiments aiming specifically at these regions, using different markers of cell death, and different time points are necessary to further study CCCI induced cell death in subcortical regions.

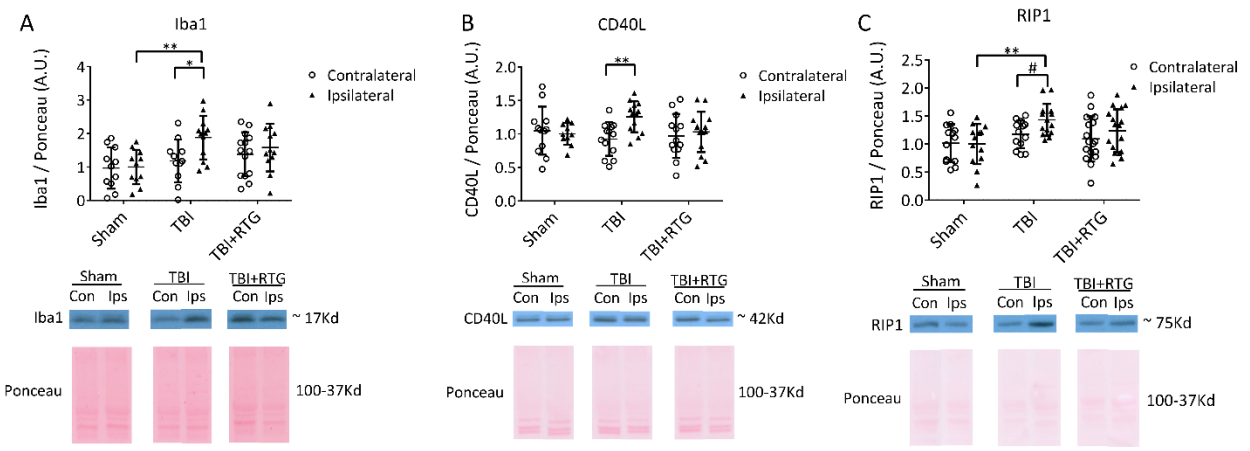

Supplementary Figure 4. Immunoblot analysis using ponceau red as an internal control. Shown are representative bands and summarized data for the same immunoblot analysis presented in Figs. 3 & 4. However, here, ponceau red staining was used as internal control for normalization of each sample. **(A)** Data for Iba1 (Sham: ipsi N=11, contra N=11; TBI: ipsi N=12, contra N=11; TBI+RTG: ipsi N=12, contra N=14). There was a significant difference between groups (Two-way ANOVA, $F_{2,70}$=5.1; p=0.009), hemisphere side ($F_{1,70}$=4.2; p=0.04), but no interaction between these two factors ($F_{2,70}$=1.6; p=0.19). There was a significant difference between contralateral and ipsilateral side only within TBI group (Bonferroni *post-hoc* test, t=2.6; p=0.01), with no difference between the two hemispheres within Sham (t=0.1; p=0.90) or TBI+RTG (t=0.8; p=0.42) animals. There was also a significant difference between Sham ipsilateral and TBI ipsilateral samples (t=3.3; p=0.005), with no difference between Sham and TBI+RTG ipsilateral samples (t=2.1; p=0.09) or between TBI+RTG and TBI ipsilateral samples (t=1.1; p=0.76). There was no significant difference between groups within contralateral samples (Sham X TBI, t=0.7; p=1.0 // Sham X TBI+RTG, t=1.6; p=0.33 // TBI X TBI+RTG, t=0.7; p=1.0). **(B)** Immunoblot data for CD40L (Sham: ipsi N=10, contra N=10; TBI: ipsi N=11, contra N=13; TBI+RTG: ipsi N=14, contra N=12). There was a significant difference between hemispheres (Two-way ANOVA, $F_{1,76}$=5.0; p=0.02), with no effect of treatment group ($F_{2,76}$=0.2; p=0.77) or interaction between these factors ($F_{2,76}$=1.5; p=0.22). There was a significant difference between contralateral and ipsilateral samples only within the TBI group (t=2.6; p=0.009), but not within Sham (Bonferroni *post-hoc* test. t=0.2; p=0.80) or TBI+RTG (t=1.0; p=0.31) cohorts. No significant difference was observed between any of the groups within contralateral (Sham X TBI, t=0.9; p=0.97 // Sham X TBI+RTG, t=0.6; p=1.0 // TBI X TBI+RTG, t=0.3; p=1.0) or ipsilateral (Sham X TBI, t=1.3; p=0.52 // Sham X TBI+RTG, t=0.1; p=1.0 // TBI X TBI+RTG, t=1.4; p=0.49). **(C)** Data for RIP-1 (Sham: ipsi N=13, contra N=13; TBI: ipsi N=14, contra N=13; TBI+RTG: ipsi N=17, contra N=17). There was a significant difference between the different groups (Two-way ANOVA, $F_{2,86}$=4.8; p=0.01), with no effect of brain hemisphere ($F_{1,86}$=2.9; p=0.08) or effect of interaction between these two factors ($F_{2,86}$=1.0; p=0.35). There was a significant difference between Sham and TBI animals within ipsilateral side (Bonferroni *post-hoc* test, t=3.2; p=0.005), but not within the contralateral side (t=1.1; p=0.73). There was no other difference between any of the groups between ipsilateral (Sham X TBI+RTG, t=1.8; p=0.19 // TBI X TBI+RTG, t=1.5; p=0.36) or contralateral sides (Sham X TBI+RTG, t=0.5; p=1.0 // TBI X TBI+RTG, t=0.6; p=1.0). There was also no significant difference comparing ipsilateral and contralateral samples between Sham (t=0.1; p=0.90), TBI+RTG (t=1.2; p=0.22) or TBI (t=1.9; p=0.05) groups. The results presented here are similar to the ones obtained in Figs. 3 & 4, even though proteins were normalized by the levels of a different internal control. *p<0.05; **p<0.01; #p=0.05; Data are presented as the mean and S.D.

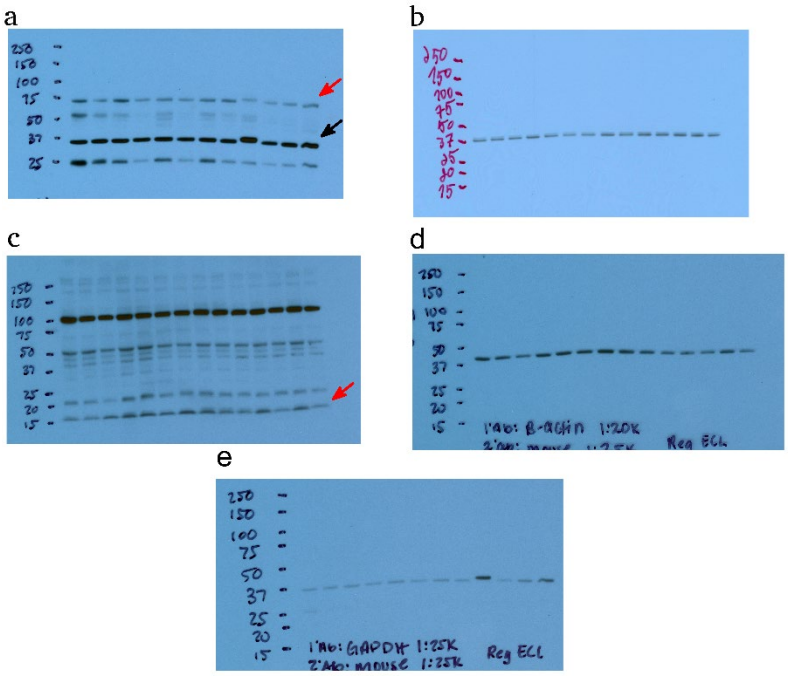

Supplementary Figure 5. Representative immunoblots. Shown are scanned images of the X-ray films from the immunoblot analysis presented in figures 3 and 4. Shown are the full images of the membranes. These images are the same images that were cropped to obtain the example bands shown in Figs. 3 & 4. Immunoblots were probed for RIP-1 (A), CD40L (B), Iba1 (C), β-actin (D) and GAPDH (E). Red arrows in this figure point to the bands of interest. The black arrow in panel (A) point to β-actin bands. This membrane was probed for both β-actin and RIP-1 as β-actin was used as internal control for RIP-1 quantification. Both bands can be seen with prolonged film exposition since the primary antibody for both was produced in the same animal species.

SUPPLEMENTAL REFERENCES

132. Spratt HM and Ju H. Statistical Approaches to Candidate Biomarker Panel Selection. *Adv Exp Med Biol* 2016; 919: 463-492. DOI: 10.1007/978-3-319-41448-5_22.

133. Aguinis H, Gottfredson R and Joo H. *Best-Practice Recommendations for Defining, Identifying, and Handling Outliers*. 2013, p.270-301.

134. Leys C, Ley C, Klein O, et al. *Detecting outliers: Do not use standard deviation around the mean, use absolute deviation around the median*. 2013, p.764–766.

135. Rousseeuw P and Croux C. *Alternatives to Median Absolute Deviation*. 1993, p.1273-1283.

136. Bland JM, Altman DG and Rohlf FJ. In defence of logarithmic transformations. *Stat Med* 2013; 32: 3766-3768. DOI: 10.1002/sim.5772.

137. McDonald JH. *Handbook of Biological Statistics 2nd Edition*. 2009.